CONTROLLABILITY ANALYSIS FOR THE FLUID CATALYTIC CRACKING PROCESS.

M. Hovd and S. Skogestad*

Chemical Engineering
University of Trondheim, NTH
N-7034 Trondheim, Norway

Presented at the AIChE Annual Meeting, Paper 145G
Los Angeles, November 17-22, 1991

Abstract

The paper illustrates a methodology for control structure selection (selection and pairing of manipulated and controlled variables) for the "lower-level" control system. We discuss the objectives of this control level and the alternative structures. To select an appropriate control structure we use as tools the existence of right half plane (RHP) transmission zeros together with the relative gain array (RGA), the frequency dependent performance relative gain array (PRGA), and the closed loop disturbance gain (CLDG). The sensitivity of the measurement selection and variable pairing with respect to changes in the operating point and parametric uncertainty is also studied. The "lower-level" control system for the Fluid Catalytic Cracking process is used as an example. Several authors have found the Kurihara control structure to be preferable to the conventional control structure. The reason for this is shown to be that RHP transmission zeros limit the achievable bandwidth for the conventional control structure. However, our analysis shows that another control structure presently used in industry has better controllability characteristics than both the conventional the Kurihara control structures.

1 Introduction

The Fluid Catalytic Cracking (FCC) process is an important process in refineries for upgrading heavy hydrocarbons to more valuable lighter products. Both decentralized controllers and more complex model predictive controllers are used to control the FCC

*Author to whom all correspondence should be addressed. E-mail: SKOGE@KJEMI.UNIT.NO, phone: 47-7-594154, fax: 47-7-591410.

process. However, when model predictive control (MPC) is used, it is usually applied on top of a lower-level decentralized control system and sends setpoint changes to the individual loops. Thus, it is important also in this case that the decentralized control system is well designed.

A schematic overview of the FCC process is shown in Fig. 1. Feed oil is contacted with hot catalyst at the bottom of the riser, causing the feed to vaporize. The cracking reactions occur while the oil vapor and catalyst flow up the riser. As a byproduct of the cracking reactions coke is formed and is deposited on the catalyst, thereby reducing catalyst activity. The catalyst and products are separated in what for historical reasons is still known as the reactor[1]. The catalyst is then stripped with steam to remove any strippable hydrocarbons, before being returned to the regenerator where the coke is burnt off in contact with air. The combustion of coke in the regenerator provides the heat needed for feed vaporization and the endothermic reaction in the riser.

In this work, the existence of right half plane (RHP) zeroes and the frequency dependent relative gain array (RGA) and closed loop disturbance gain (CLDG) are used for control structure selection, and we study the effect of structural and parametric uncertainty in the models and uncertainty in the manipulated variables on the choice of control structure for decentralized control. The use of frequency dependent RGA and CLDG are explained by Skogestad and Hovd (1990) and Hovd and Skogestad (1991).

2 The "lower-level" control problem (regulatory)

The *overall control objective* is to maintain safe operation while keeping the operating conditions close to the economically optimal conditions. This objective is commonly achieved using a hierarchical control system, with different tasks assigned to each level in the hierarchy. In this paper we consider what is typically the lowest level in this control hierarchy, which in industry is commonly called the distributed control system (DCS). Usually, this is a decentralized control system which keeps a set of measurements at given setpoints. This is a cascaded control system where the value of these setpoints are determined by the operator or by higher levels in the control hierarchy. In the following we shall use the abbrevation DCS to denote the lower-level control system.

The primary task of the lower-level control system is to perform regulatory control at the loop level. At the intermediate level (supervisory control level) there is is usually a model based system which uses a multivaraiable process model to calculate how the plant should be operated to optimize some objective which takes into account constraints in measurements and manipulated variables. The top level in the control hierarchy is a plant wide optimization. This optimization is usually steady state and is performed offline at regular intervals. A schematic representation of such a control hierarchy is depicted in Fig. 2. The lower-level (DCS) control system should fulfill the following objectives:

O1. It should provide a sufficient quality of control to enable a trained operator to keep the plant running safely without use of the higher levels in the control system. For

[1] With less active catalysts, the residence time in the reactor was needed to perform the cracking. With modern catalysts, the catalyst and products must be separated as quickly as possible at the riser exit to prevent overcracking.

example, this sharply reduce the need for providing costly backup systems for the higher levels of the control hierarchy in case of failures.

O2. It should be simple to understand and tune. Thus, in most cases simple decentralized control loops are used at this level.

O3. It should make it possible to use relatively simple (at least in terms of dynamics) models at the higher level. We want to use relatively simple models because of reliability and the prohibitive costs involved in obtaining and maintaining a detailed dynamic model of the plant, and because complex dynamics will add to the computational burden on the higher level control system. This may be achieved by letting the lower-level control system take care of the regulatory tasks. This may also provide for local linearization, for example, by using a cascade on a valve to avoid the nonlinear valve characteristics.

O4. It should make it possible to use longer sampling intervals at the higher levels of the control hierarchy which significantly reduces the need for computing power at this level. Preferably, the time scales of the lower-level and higher-level control system should be separated such that response of the low-level control system, as seen from the higher level, is almost immediate.

As a consequence of the objectives listed above, additional objectives for the DCS arise:

O5. It should provide for fast control when this is needed for some variables.

O6. It must be able to follow the setpoints set by the higher levels in the control hierarchy. The setpoints of the lower loops are the manipulated variables for the higher levels in the control hierarchy, and we want to be able to change these variable as directly and with as little interaction as possible. Otherwise, the higher level will need a model of the dynamics and interactions of the outputs from the lower level control system.

O7. It should provide for local disturbance rejection. This follows from objective 6 above, since we want to be able to keep the lower-level on their desired setpoints. As disturbances we must also inclused the "unused" manipulated variables which are adjusted directly by the higher-level control system.

O8. It should be designed such that the remaining control problem does not contain unneccessary performance limitations such as RHP-zeros, large RGA elements, or strong sensitivity to disturbances. The "remaining control problem" is the control problem as seen from the higher level which has as manipulated inputs the "unused" manipulated inputs and the setpoints to the lower-level control system. By "unnecessary" is meant limitations that does not exist in the original problem formulation without the lower-level control system in place.

In this paper we will primarily consider objectives 5, 6 and 7. These objectives are related to the "controllability" of the lower level control system. Objective 2 is automatically fulfilled since we are only considering a fully decentralized lower level control system.

Note that also the lower level control system itself may include cascaded loops. For example, one often cascades the valve position to a flow measurement such that flow becomes the manipulated input rather than the valve position. To fulfill these objectives for the lower level control system one must make the following structural decisions (of course, the controller design comes in addition):

D1. Selection of controlled variables, i.e., outputs y (control objectives for the lower-level control system).

These variables include *primary* and *secondary* controlled variables. The primary outputs are variables which are important to control in themselves, also in terms of the overall control objective. Typically, this includes objectives where reasonably fast control is needed (see objective 5 above), such as liquid levels, certain temperatures and sometimes pressure. The secondary outputs are usually easily measured variables which are selected to meet the objectives mentioned above, for example, temperatures and pressures at selected locations in the process. The problem of selecting the output variables for the lower level control system is therefore closely related to the issue of measurement selection.

D2. Selection of manipulated variables, inputs u, to pair with the chosen controlled variables, y.

These selected inputs will be a subset of all possible manipulated inputs, and the remaining "unused" variables will be manipulated inputs available for the higher levels.

D3. Pairing of the chosen controlled and manipulated variables.

The choice of pairing will influence the effect of interactions and disturbances, as well as the systems ability to tolerate failure of one or more loops in the decentralized control system.

More generally, the unused input variables may be unused degrees of freedom, which need not be physical manipulated inputs, but rather combinations of these. This may be done by redefining the manipulated inputs using some input transformation (usually static). Again, distillation column control provides a good example. Here, there are two flows leaving the condenser, reflux L and distillate D. Both these manipulated variables affect the condenser level and the top composition. The level control is performed by the lower-level control system and this leaves one degree of freedom for the remaining composition control system. This degree of freedom may be L (in which case D is used for level control), D (in which case L is used for level control), or L/D (in which case some combination of L and D, for example, L or L+D, is used for level control). The last example is illustrated in Fig. X.

3 Measures for evaluating controllability

Right half plane transmission zeros. A right half plane (RHP) transmission zero of $G(s)$ limits the achievable bandwidth of the plant. This holds regardless of the type of

controller used (e.g., Morari and Zafiriou, 1989). The reason is that with a RHP-zero the controller can not invert the plant and perfect control is impossible. Thus plants with RHP transmission zeros within the desired bandwidth should be avoided.
In the multivariable case a RHP-zero of $G(s)$ does not imply that the matrix elements, $g_{ij}(s)$, have RHP-zeros. Conversely, the presence of RHP-zeros in the elements does not necessarily imply a RHP-zero of $G(s)$. If we use a multivariable controller then RHP-zeros in the elements do not imply any particular problem. However, if decentralized controllers are used, then we generally avoid pairing on elements with "significant" RHP-zeros (RHP-zeros close to the origin), because otherwise this loop may go unstable if left by itself (with the other loops open).[2]

Relative gain array. The relative gain array (RGA) has found widespread use as a measure of interaction and as a tool for control structure selection for single-loop controllers. It was first introduced by Bristol (1966). It was originally defined at steady-state, but it may easily be extended to higher frequencies (Bristol, 1978). Shinskey (1967,1984) and several other authors have demonstrated practical applications of the RGA. Important advantages with the RGA is that it depends on the plant model only and that it is scaling independent. For $n \times n$ plants $G(s)$ the RGA matrix can be computed using the formula

$$\Lambda(s) = G(s) \times (G^{-1}(s))^T \tag{1}$$

where the $\times$ symbol denotes element by element multiplication (Hadamard or Schur product). An important usage of the RGA is that pairing on negative *steady-state* relative gains should be avoided (Grosdidier and coworkers, 1985). The reason is that with integral control this yields instability of either 1) the overall system, 2) the individual loop, or 3) the remaining system when the loop in question is removed. It is also established that plants with large RGA-values, in particular at high frequencies, are fundamentally difficult to control irrespective of the controller used (poor controllability).

PRGA. One inadequacy of the RGA (eg., McAvoy, 1983, p. 166) is that because it only measures two-way interactions (e. g. $\Lambda = I$ for a triangular plant), may indicate that interactions is no problem, but significant one-way coupling may exist. To overcome this problem we introduce the frequency dependent performance relative gain array (PRGA). The PRGA matrix is defined as

$$\Gamma(s) = \tilde{G}(s)G(s)^{-1} \tag{2}$$

where $\tilde{G}(s)$ is the matrix consisting of only the diagonal elements of $G(s)$, i.e., $\tilde{G} = diag\{g_{ii}\}$. The matrix Γ was originally introduced at steady-state by Grosdidier (1990) in order to understand the effect of directions under decentralized control. The elements of Γ are given by

$$\gamma_{ij}(s) = g_{ii}(s)[G^{-1}(s)]_{ij} = \frac{g_{ii}(s)}{g_{ji}(s)}\lambda_{ji}(s) \tag{3}$$

Note that the diagonal elements of RGA and PRGA are identical, but otherwise PRGA does not have all the nice algebraic properties of the RGA. PRGA is independent of *input*

[2] Usually the main reason for using a decentralized control system in the first place is to allow for loops to be operated independently.

scaling, that is, $\Gamma(GD_2) = \Gamma(G)$, but it depends on output scaling. This is reasonable since performance is defined in terms of the magnitude of the outputs.

Closed loop disturbance gain. A disturbance measure related to the RGA, the closed loop disturbance gain (CLDG), was recently introduced by Skogestad and Hovd (1990). For a disturbance k and an output i, the CLDG is defined by

$$\delta_{ik}(s) = g_{ii}(s)[G(s)^{-1}G_d(s)]_{ik} \tag{4}$$

The reason for the name CLDG will become clear later. A matrix of CLDG's may be computed from

$$\Delta = \{\delta_{ik}\} = \tilde{G}G^{-1}G_d \tag{5}$$

The CLDG is scaling dependent, as it depends on the expected magnitude of disturbances and outputs. Actually, this is reasonable since CLDG is a performance measure, which generally are scaling dependent.

Performance relationships for decentralized control. Assume the controller $C(s)$ is diagonal with entries $c_i(s)$. (see Fig. 3). This implies that after the variable pairing has been determined, the order of the elements in y and u has been arranged so that the plant transfer matrix $G(s)$ has the elements corresponding to the paired variables on the main diagonal. Let $y(s)$ denote the output response for the overall system when all loops are closed and let $e(s) = y(s) - r(s)$ denote the output error. The closed loop response becomes

$$e(s) = -S(s)r(s) + S(s)G_d(s)d(s); \quad S = (I + GC)^{-1} \tag{6}$$

where $S(s)$ is the sensitivity function for the overall system, and $d(s)$ denotes the disturbances. The Laplace variable s is often omitted to simplify notation.
At low frequencies ($\omega < \omega_B$) we usually have (Skogestad and Hovd (1990), Hovd and Skogestad (1991)) $S \approx (GC)^{-1} = C^{-1}\tilde{G}^{-1}\tilde{G}G^{-1} = (\tilde{G}C)^{-1}\tilde{G}G^{-1} \approx \tilde{S}\tilde{G}G^{-1}$ and we get

$$e \approx -\tilde{S}\tilde{G}G^{-1}r + \tilde{S}\tilde{G}G^{-1}G_d d; \quad \omega < \omega_B \tag{7}$$

Here we recognize the PRGA ($\tilde{G}G^{-1}$) and the CLDG ($\tilde{G}G^{-1}G_d$). When we consider the effect of a setpoint change r_j and a disturbance d_k on the offset e_i this gives

$$e_i \approx -\frac{\gamma_{ij}}{g_{ii}c_i}r_j + \frac{\delta_{ik}}{g_{ii}c_i}d_k; \quad \omega < \omega_B \tag{8}$$

From (8) we see that the ratio $\gamma_{ij}/(g_{ii}c_i)$ gives the magnitude of the offset in output i to a unit setpoint change for output j. This ratio should preferably be small. That is, on a conventional magnitude Bode plot (log-log), the curve for $|\gamma_{ij}|$ should lie below $|g_{ii}c_i|$ at frequencies where we want small offsets. For process control disturbance rejection is usually more important than setpoint tracking. From (8) we see that the ratio $\delta_{ik}/(g_{ii}c_i)$ gives the magnitude of the offset in output i to a disturbance d_k. That is, the curve for $|\delta_{ik}|$ should lie below $|g_{ii}c_i|$ at frequencies where we want small offsets. A plot of $|\delta_{ik}(j\omega)|$ will give useful information about which disturbances k are difficult to reject.
Assume that G and G_d have been scaled such that 1) the expected disturbances, $|d_k(j\omega)|$, are less or equal to one at all frequencies, and 2) the outputs, y_i are such that the allowed

errors, $|c_i(j\omega)|$, are less or equal to one. *In this case the frequency where* $|\delta_{ik}(j\omega)|$ *crosses one, directly corresponds to the minimum bandwidth needed in loop* i *to reject disturbance* k. It is preferable that this frequency is low in order to avoid stability problems for the individual loops.

Limitations of (8). The main limitation with (8) is that it applies only to lower and intermediate frequencies. Furthermore, the issue of stability is not addressed. Another limitation is the assumption that all diagonal elements in $G(s)$ are nonzero. In particular, it is obvious that relations involving $|g_{ii}c_i|$ in the denominator are not meaningful when $g_{ii} = 0$. These issues are addressed in Hovd and Skogestad (1991).

3.1 Summary of controllability rules

Let us at this point summarize some results we shall use in this paper:

Rule 1. Avoid plants (designs) with RHP transmission zeros within the desired bandwidth (i. e. RHP transmission zeros at low frequencies are bad).

Rule 2. Avoid plants (designs) with large RGA-values (in particular at frequencies near cross-over). This rule applies for any controller, not only to decentralized control (Skogestad and Morari, 1987b).

Rule 3. Avoid *pairings* ij with negative values of the steady-state RGA, $\lambda_{ij}(0)$ (Grosdidier et al., 1985).

Rule 4. Prefer *pairings* ij where $g_{ij}(s)$ puts minimal restrictions on the achievable bandwidth for this loop, that is, avoid pairings with RHP-zeros in $g_{ij}(s)$. The rule follows from (8) above in order to satisfy performance and at the same time have stability of the individual loop. Rule 4 is the conventional rule of pairing on variables "close to each other".

Rule 5. For decentralized control avoid control structures (an entire *set* of *pairings*) with large values of $|\delta_{ik}|$ in the crossover region, and in particular if the achievable bandwidth for the corresponding loop i is restricted (because of $g_{ii}(s)$, see rule 4) (the rule follows from (8) above).

4 FCC operating modes

The FCC process can be operated in two distinct modes:

1) In the partial combustion mode, large amounts of both CO and CO_2 are formed when the coke is burnt in the regenerator. If there are significant amounts of oxygen leaving the regenerator dense bed, this will react with the CO to form CO_2 in the zone above the regenerator dense bed, or in the regenerator cyclones and downstream piping. This phenomenon is known as "afterburning". The combustion of CO to CO_2 is a strongly exothermic reaction, therefore a large temperature rise will occur if there are significant

amounts of oxygen leaving the regenerator dense bed. It is therefore necessary to control the afterburning to avoid violating metallurgical temperature limits for the regenerator cyclones or downstream piping. The CO rich regenerator flue gas can be sent to a CO boiler where high pressure steam is produced.

2) In the complete combustion mode, little CO leaves the regenerator dense bed because excess quantities of air is supplied so that most of the CO formed by the combustion of coke is oxidized to CO_2 within the regenerator dense bed. Special catalysts which promote the oxidation of CO to CO_2 may also be used (Rheaume, 1976). When operating in the complete combustion mode afterburning is therefore not such a serious concern. The heat released by the combustion of CO to CO_2 can be more easily accommodated in the regenerator dense bed than above the dense bed and in the cyclones, because the large mass of catalyst present in the dense bed makes the resulting temperature rise smaller. However, it is not always possible to operate an FCC unit in the complete combustion mode, especially if the feed oil has a large coke production tendency. There is also an economic incentive for operating in the partial combustion mode, as the heat recovered in the CO boiler is valuable.

5 Models of the FCC process used in this work

The models used in this work derive in the main part from the model proposed by Lee and Groves (1985) for the partial combustion mode. This model augments the regenerator model of Errazu and coworkers (1979) with the riser model of Shah and coworkers (1977).

5.1 Riser model

A static model is used for the riser. We use an ideal plug flow model and the three lump kinetic scheme of Weekman and Nace (1970). In this scheme the feed is gas oil, which can crack to gasoline or light gases/coke.
Material balance for gas oil:

$$\frac{dy_f}{dz} = -K_1 y_f^2 [COR] \Phi t_c \tag{9}$$

Material balance for gasoline:

$$\frac{dy_g}{dz} = (\alpha_2 K_1 y_f^2 - K_3 y_g)[COR] \Phi t_c \tag{10}$$

where

$$K_1(\Theta) = k_1 exp(\frac{-E_f}{RT_0(1+\Theta)}) \tag{11}$$

$$K_3(\Theta) = k_3 exp(\frac{-E_g}{RT_0(1+\Theta)}) \tag{12}$$

$$\Theta = (T - T_0)/T_0 \tag{13}$$

$$\Phi = \phi_0 exp(-\alpha t_c [COR] z) \tag{14}$$

$$\phi_0 = 1 - m C_{rc} \tag{15}$$

Here $K_1 y_f^2[COR]$ represents the kinetics for the cracking of gas oil and $K_3 y_g[COR]$ the kinetics for cracking of gasoline. Φ represents the deactivation of the catalyst caused by coke deposition, of which o_0 represents the reduction in catalyst activity caused by the coke remaining on the catalyst after regeneration. t_c is the residence time in the riser, and $\alpha_2 = k_2/k_1$ is the fraction of the cracked gas oil which cracks to gasoline.
The catalyst to oil ratio $[COR]$, which was omitted by Lee and Groves, is reintroduced into Φ in order to be consistent with the original model of Shah et al. A correlation taken from Kurihara (1967) is used to estimate the amount of coke produced.

$$C_{cat} = k_c \sqrt{\frac{t_c}{C_{rc}^N} exp(\frac{-E_{cf}}{RT_1})} \tag{16}$$

The amount of coke on the catalyst leaving the riser is thus

$$C_{sc} = C_{rc} + C_{cat} \tag{17}$$

The energy balance yields:

$$\frac{d\Theta}{dz} = \frac{\Delta H_f F_f}{T_0(F_s c_{ps} + F_f c_{po} + \lambda F_f c_{pd})} \frac{dy_f}{dz} \tag{18}$$

5.2 Regenerator models

When modeling the regenerator it is common to assume that the temperature and the amount of coke on the catalyst is uniform throughout the regenerator. In the model used in this paper, oxygen is also assumed to be *uniformly distributed* in the regenerator dense bed, as Errazu and coworkers (1979) found that operational data well can be well described assuming uniform distribution of oxygen in the regenerator. Some authors use the assumption that the oxygen moves in perfect plug flow through the dense bed (eg. Kurihara, 1967, Krishna and Parkin, 1985). At the end of the paper we will comment on how the assumptions about oxygen flow pattern affect our conclusions.
The regenerator is described by the following equations. Balance for coke on regenerated catalyst:

$$W\frac{d}{dt}C_{rc} = F_s(C_{st} - C_{rc}) - R_{cb} \tag{19}$$

Energy balance:

$$W c_{ps}\frac{d}{dt}T_{rg} = T_{st}F_s c_{ps} + T_a F_a c_{pa} - T_{rg}(F_s c_{ps} + F_a c_{pa}) - \Delta H_{cb} R_{cb}/M_c \tag{20}$$

where ΔH_{cb} depends both on the temperature and σ, the ratio of CO_2 to CO produced (Errazu and coworkers 1979). Here n denotes the average coke composition CH_n. The concentration of oxygen in the regenerator dense bed is given by a material balance

$$W_a\frac{d}{dt}O_d = \frac{F_a}{M_a}(O_{in} - O_d) - \frac{(1+\sigma)n + 2 + 4\sigma}{4(1+\sigma)}\frac{R_{cb}}{M_c} \tag{21}$$

The rate of coke combustion is given by

$$R_{cb} = k_{cb} exp(\frac{-E_{cb}}{RT_{rg}}) O_d C_{rc} W \tag{22}$$

Overall this yields a third order model for the regenerator, with C_{rc}, T_{rg} and O_d as states. We want to use the regenerator cyclone temperature as an output, and include the afterburning of CO to CO_2 in the dilute phase in the regenerator by using a simple equation taken from Kurihara (1967)

$$T_{cy} = T_{rg} + c_t O_d \tag{23}$$

For Eq. (23) to be reasonable, there must be an excess of CO over O_2 in the gas leaving the regenerator dense bed, that is, Eq. (23) is only valid in the partial combustion mode. When using Eq. (23), controlling $\Delta T_{rg} = T_{cy} - T_{rg}$ (the temperature rise from regenerator dense bed to regenerator cyclones) is equivalent to controlling O_d (the amount of oxygen leaving the regenerator dense bed).

5.3 Reactor (stripper) model

As explained previously, no reaction occurs in the "reactor", which in modern FCC's is simply used as a stripping vessel, where volatile hydrocarbons are stripped from the catalyst using steam. The flowrate of stripping steam is small compared to the flowrates of catalyst and feed oil, and the effect of the steam on the heat balance of the reactor is therefore ignored. Assuming the stripping is effective, the only effect of the reactor will be to introduce a lag between the riser exit and the catalyst return to the regenerator. This lag is modeled using an ideal mixing tank. The balances for coke and energy yield.

$$W_{st}\frac{d}{dt}C_{st} = F_s(C_{sc} - C_{st}) \tag{24}$$

$$W_{st}c_{ps}\frac{d}{dt}T_{st} = F_s c_{ps}(T_1 - T_{st}) \tag{25}$$

The catalyst holdup in the reactor W_{st} is assumed to be kept constant by perfect control. This means that the flowrate of spent catalyst from the reactor to the regenerator, $\hat{F}_s$, equals the flowrate of regenerated catalyst, F_s.

5.4 Complete combustion mode

The above model has been adjusted to describe the complete combustion mode as follows:

1. The ratio of CO_2 to CO produced in the regenerator, σ, is fixed to a high value, such that there is an excess of O_2 over CO in the gas leaving the regenerator dense bed. Then the oxygen concentration in the flue gas, O_f, will be approximately equal to the oxygen concentration in the gas leaving the regenerator dense bed, O_d.

2. The air rate to the regenerator, the coke production rate (k_c) and the feed oil temperature have been adjusted in order to achieve energy balance in the desired operating region.

3. Finally we have adjusted the model parameters to obtain the same signs for the steady state gains as observed by Grosdidier (1990a):

$$\begin{bmatrix} T_1 \\ O_d \end{bmatrix} = \begin{bmatrix} + & - \\ - & + \end{bmatrix} \begin{bmatrix} F_s \\ F_a \end{bmatrix} \tag{26}$$

These signs for the steady state gains should be obtained in the region of the following operating conditions (Grosdidier, 1990b):
Flue gas oxygen concentration: 0.4-1.4 mole%
Regenerator dense bed temperature: 989-1009 K
In order to obtain the desired signs for the steady state gains it has been necessary to reduce the activation energy for coke formation, E_{cf} and to remove the dependency of the coke production on the amount of coke on regenerated catalyst, C_{rc} [3].

5.5 Parameter values

The parameter values used are given in the nomenclature section. The values used are taken from Ljungquist (1990), who has slightly modified the values given by Lee and Groves. The value of c_t is taken from Kurihara (1967).
As explained above, we have for the complete combustion mode adjusted the values of E_{cf}, k_c and N.

5.6 Constraints

The optimal operating point for an FCC usually lies at one or several constraints. The control structure which allows operation closest to the constraints is therefore preferable. The location of the optimal operating point, and consequently the importance of the different constraints can vary depending on the feed characteristics and the desired product split. Different control structures may thus be preferable at different operating points, but it is not realistic to expect the control structure to be reconfigured when the operating conditions are changed.
Common constraints include:

- Maximum regenerator cyclone temperature constraint. This constraint is usually important in the partial combustion mode, and is determined by the metallurgical properties of the cyclones.

- Minimum flue gas oxygen concentration constraint. This constraint is important in the complete combustion mode, as a sufficient concentration of oxygen in the flue gas ensures virtually complete combustion of CO to CO_2 within the regenerator dense bed, and therefore ensures that afterburning is avoided. Thus sufficient oxygen in the flue gas also ensures that the concentration of CO in the flue gas is within environmental limits.

[3] This seems reasonable since FCC's operating in the complete combustion mode commonly achieve very good regeneration with very small amounts of coke on regenerated catalyst (Rheaume et al., 1976). For these low amounts of coke on regenerated catalyst, Eq. (16) would predict both a very large coke production and a very strong dependence of the coke production on the amount of coke on regenerated catalyst. This does not appear realistic, and we have therefore set $N = 0$ in our studies of the complete combustion mode of operation.

- Maximum wet gas compressor capacity. The wet gas compressor is situated downstream of the FCC unit, and compresses the wet gases produced in the FCC for transportation to downstream gas treatment plants.

- Maximum air blower capacity. The air blower provides the air needed for the combustion in the regenerator.

For a more complete description of the constraints encountered in the operation of FCC's, see Grosdidier et al. (1991).

5.7 Variable classification

Independent variables (u's and d's). We will consider the following six independent variables:

- F_s - The flowrate of regenerated catalyst from regenerator to reactor.
- F_a - The flowrate of air to the regenerator.
- k_c - The coke production rate factor (i. e., feed oil composition)
- T_f - The feed oil temperature.
- F_f - The total feed oil flowrate (both fresh and recycled oil).
- T_a - The air temperature.

We have not included the spent catalyst flowrate from stripper to regenerator, $\hat{F}_s$ as we have assumed that it is used to control the catalyst holdup in the stripper, W_{st}. Other possible independent variables which are not included here include the fraction of dispersion steam, λ, and the stripping steam flowrate (not included in the model). All the six independent variables above may be used as manipulated variables (u's) for control, but in most cases we will only use two: the regenerated catalyst flowrate, F_s and the air flowrate F_a. The remaining independent variables may then be regarded as disturbances (d's).
The variables k_c, T_f and F_f are all related to the oil feed. k_c is the coke production rate factor and depends on the feed composition. (Immediately downstream of the FCC there is a distillation column which separates the products from the cracking reactions. The heavy fraction from the distillation column (commonly called "slurry") has a large coke producing tendency. The coke production rate factor can therefore be changed indirectly by changing the amount of slurry which is recycled to the riser). The air temperature T_a is generally a disturbance since there is usually no air preheater.

Measurements. Typically, the following measurements are available:
Partial combustion mode:

- T_1 - The riser exit temperature.
- T_{rg} - The regenerator dense bed temperature.

- T_{cy} - The regenerator cyclone temperature.

Complete combustion mode:

- T_1 - The riser exit temperature.
- T_{rg} - The regenerator dense bed temperature.
- $O_f \approx O_d$ - The oxygen concentration in the flue gas

Controlled variables (y's)
The product distribution is determined by the reaction conditions inside the riser, which are therefore very important for the economic performance of the FCC process. Both T_1 and T_{rg} are related to the conditions in the riser. There is an incentive to control *both* T_1 and T_{rg}, as the product distribution depends both on the temperature inside the riser and the catalyst to oil ratio. For a given valus of T_1, a high value for T_{rg} implies a low catalyst to oil ratio.
The need to control afterburning in the partial combustion mode and to avoid afterburning in the complete combustion mode should be obvious.
Thus, the controlled variables considered in this work are:
Partial combustion mode:
Primary variable: T_{cy} or $\Delta T_{rg} = T_{cy} - T_{rg}$.
Secondary variables: T_1 and T_{rg}
Complete combustion mode:
Primary variable: O_f.
Secondary variables: T_1 and T_{rg}

5.8 Control structure alternatives

3×3 control systems. As discussed above we may want to control three outputs. For the partial combustion mode we have

$$y^3 = (T_1, T_{rg}, T_{cy})^T \tag{27}$$

We will consider the following alternative manipulated variables:

$$u_1^3 = (F_s, F_a, k_c)^T \tag{28}$$

$$u_2^3 = (F_s, F_a, T_f)^T \tag{29}$$

Here we assume that the unit is operating at some maximum capacity limit such that F_f is not available as a manipulated variable for temperature control. For example, F_f may be restricted by the maximum capacity of the downstream wet gas compressor.
Computing the RGA for the resulting 3×3 system shows that the use of u_2^3 gives large RGA values (largest steady state RGA element of 24), showing that this choice of manipulated variables gives a system with strong interactions. Choosing u_1^3 as manipulated variables results in much weaker interactions (largest steady state RGA element of 2.0).

For the complete combustion mode we have

$$y^3 = (T_1, T_{rg}, O_f)^T \tag{30}$$

whereas u_1^3 and u_2^3 are the same as in the partial combustion mode. Using u_1^3 we find that the largest element of the steady state RGA is 7.2, whereas using u_2^3 we find that the largest steady state RGA element is 37. Thus u_1^3 seems to be a better choice of manipulated variables than u_2^3 also in the complete combustion mode, and we conclude that the feed temperature is a poor manipulator.

2×2 control systems: Selection of controlled variables. Although the 3×3 control problem is interesting, we will in the following consider the 2×2 problem, with F_s and F_a as manipulated variables.
Restricting our attention to the 2×2 control problem allows us to compare and contrast our results with the results of previous authors, and will give a good illustration of the effect measurement selection can have on plant controllability. Furthermore, the output variables T_1 and T_{rg} are strongly coupled, and good control of one will in many cases also limit the offset in the other variable. There is thus probably little need to control both T_1 and T_{rg} in order to fulfill the objectives for the lower level control system given above. In the following we will use

$$u = (F_s, F_a)^T \tag{31}$$

as manipulated variables. These two manipulated variables are always used for 2×2 control systems for FCC's, because of their strong and direct effect on the process conditions. The remaining independent variables k_c, T_f, F_f and T_a will in the following be considered as disturbances. In the partial combustion mode we will investigate the following four choices of controlled variables:

1. $y_C = (T_1, \Delta T_{rg})^T$. This corresponds to the *conventional control structure*, which uses F_s to control T_1 and F_a to control ΔT_{rg}. It appears to have been described first by Pohlenz (1963), but the name is due to Kurihara (1967).

2. $y_K = (T_{rg}, \Delta T_{rg})^T$. This corresponds to the *Kurihara control structure* (Kurihara, 1967), which uses F_a to control T_{rg} and F_s to control ΔT_{rg}.

3. $y_{AK} = (T_{rg}, T_{cy})^T$. We have chosen to call this the *alternative Kurihara* control structure, as the elements of y_{AK} are linear combinations of the elements of y_K.

4. $y_H = (T_1, T_{cy})^T$. We call this the *Hicks control structure* as it was first proposed by Hicks (1966), who used F_s to control T_1 and F_a to control T_{cy}. According to Grosdidier (1990a) this is the control structure which is presently preferred in industry.

For the complete combustion mode we will investigate the following two choices of controlled variables:

1. $y_{CC} = (T_1, O_f)^T$. Although Pohlenz (1963) and Kurihara (1967) considered only operation in the partial combustion mode, we will call this the *conventional control structure for the complete combustion mode*, because of its obvious similarity in the

choice of controlled variables with the conventional control structure for the partial combustion mode (c. f. Eq. (23)). According to Grosdidier (1990) this is also the control structure which is used in industry for controlling FCC's in the complete combustion mode.

2. $y_{KC} = (T_{rg}, O_f)^T$. We will call this the *Kurihara control structure for the complete combustion mode* because of the similarity in the choice of controlled variables with the Kurihara control structure in the partial combustion mode.

6 Analysis of FCC models

The following three sections will address:

- Choice of controlled variables. How does the choice of controlled variables affect controllability.
- Pairing of controlled and manipulated variables for decentralized control.
- Effect of operating point. Does the control system depend on changes in the operating conditions?
- Sensitivity to parametric uncertainty. Do changes in parameter values lead to different conclusions?
- Sensitivity to input uncertainty. The actual moves in the manipulated variables will not be exactly equal to those calculated by the controller. Does this influence performance?
- Disturbance rejection. Using the CLDG explained in section 3, we will investigate the effect of disturbances on the FCC when decentralized control is used.
- Effect of model features. Which features of the models are important for making decisions about the control of the FCC process?

These points will be examined for both the partial combustion and complete combustion modes.
In the following we assume that a decentralized control system is used and that the transfer function matrices have been arranged to give the paired elements on the diagonal. The word "RGA" or "RGA's" will refer to the diagonal elements of the RGA-matrix of $G(s)$, which are identical since $G(s)$ is a 2×2 matrix.

7 Partial combustion mode.

7.1 Selection of controlled variables.

1) Conventional control structure, $y_C = (T_1, \Delta T_{rg})^T$.
For this choice of controlled variables we get a transfer function matrix with an RHP

transmission zero in the frequency range $0.02 - 0.01$ [rad/min]. This RHP transmission zero will seriously limit the achievable bandwidth, and only slow control is possible. This choice of controlled variables will therefore be discarded.

2) Kurihara control structure, $y_K = (T_{rg}, \Delta T_{rg})^T$.
For this choice of controlled variables we get an RHP transmission zero at approximately $0.2 - 0.3$ [rad/min]. This is one decade higher than for the conventional control structure, and it probably does not seriously limit the achievable bandwidth. This result is in accordance with the results of Kurihara (1967) and Lee and Groves (1985), who found the Kurihara control structure to be preferable to the conventional control structure.

3) Alternative Kurihara control structure, $y_{AK} = (T_{rg}, T_{cy})^T$.
For this choice of controlled variables we get the same result as for the Kurihara control structure, an RHP transmission zero at approximately $0.2 - 0.3$ [rad/min]. This is as expected, since the measurements for the alternative Kurihara control structure are linear combinations of the measurements for the Kurihara control structure ($T_{cy} = T_{rg} + \Delta T_{rg}$).

4) Hicks control structure, $y_H = (T_1, T_{cy})^T$.
For this choice of controlled variables we get no RHP transmission zero. This means that there is no inherent bandwidth limitation in either of the models, and the bandwidth will be limited solely by unmodeled effects and uncertainty.

The existence and location of RHP transmission zeros is a fundamental measure of controllability, as an RHP transmission zero will limit the achievable bandwidth for any type of controller. Our analysis of RHP zeros clearly indicate that T_{cy} and T_1 should be chosen as controlled variables. Present industrial practice is also to control these two variables (Grosdidier, 1990a). It can also be argued that controlling T_{cy} and T_1 is the best choice with respect to the constraints:

- Controlling T_{cy} avoids exceeding the metallurgical temperaure limit in the regenerator cyclones.
- The amount of wet gases produced is a strong function of the riser exit temperature, T_1. Controlling T_1 therefore helps ensuring that the wet gas compressor operating limits are not exceeded. Controlling T_{rg} instead of T_1 would not have the same beneficial effect on the operation of the wet gas compressor.

Based on the results in this section, we will concentrate on the Hicks control structure, which has T_{cy} and T_1 as controlled variables.

7.2 Pairing of controlled and manipulated variables.

The RGA for the pairing $T_1 - F_s$, $T_{cy} - F_a$, proposed by Hicks (1966), is approximately 1 for frequencies higher than ca. 0.1 [rad/min]. We therefore choose this pairing, as our desired bandwidth is higher than 0.1 [rad/min].

7.3 Effect of changes in the operating point

The transfer function matrix G_P for the Hicks structure is defined by

$$\begin{bmatrix} T_1 \\ T_{cy} \end{bmatrix} = G_P \begin{bmatrix} F_s \\ F_a \end{bmatrix} \tag{32}$$

Although a number of operating points ("cases") have been studied, our findings can be illustrated by the two cases in Table 1.

The results on *selection of controlled variables* appear unaffected by changes in the operating point, as we have not found any operating point with an RHP transmission zero for the transfer function matrix with T_1 and T_{cy} as controlled variables. The RHP transmission zeros found for the other possible choices of controlled variables are also found when the operating point is changed, although their locations do vary somewhat.

The *choice of pairing* also appears insensitive to changes in the operating point, as the RGA at steady state is positive for the operating points studied, and is close to 1 in our desired bandwidth region.

7.4 Sensitivity to parametric uncertainty

Due to the large number of parameters in the models, the sensitivity to parameter uncertainty has not been exhaustively researched. The objective of this section is to investigate whether small errors in the parameters can have consequences for control performance, and whether parametric uncertainty therefore should be considered in the process of control structure selection.

The results on *selection of controlled variables* appear unaffected by parametric uncertainty also. We have not found any parameter change which causes an RHP transmission zero with T_1 and T_{cy} as controlled variables. Again, the RHP transmission zeros found for the other possible choices of controlled variables are also found when parameters are changed, although their locations do vary somewhat.

In general, we have found G_P to be relatively insensitive to parametric uncertainty. However, increasing k_{cb} from $2.077 \times 10^8 s^{-1}$ to $2.4 \times 10^8 s^{-1}$ together with a slight decrease in F_s changes the sign of the steady state gain from F_a to T_{cy} from positive to negative, and makes the steady state RGA negative. This illustrates that parametric uncertainty can affect our conclusions on the choice of pairing.

7.5 Disturbances

The effect of disturbances have been investigated using the closed loop disturbance gain (CLDG) explained above. Based on the results in the previous sections, we will here only consider the pairing $T_1 - F_s$, $T_{cy} - F_a$. The transfer functions were scaled such that output errors, $e_i = y_i - r_i$, of magnitude 1 corresponds to

1. Riser exit temperature, T_1: 3 K
2. Regenerator cyclone temperature, T_{cy}: 2 K

and such that disturbances, z_k, of magnitude 1 correspond to

1. Feed oil temperature, T_f: 5 K
2. Air temperature, T_a: 5 K
3. Feed oil flowrate, F_f: 4 kg/s (ca. 10%)
4. Feed oil composition, expressed by the coke production rate factor k_c: 2.5 % relative to original value.

The frequency-dependent CLDG's for case 1 (Table 1) are shown in figure 4. The curves for case 2 are very similar. The CLDG's consistently predict that disturbance $k = 3$ in the feed oil flowrate, F_f, is most difficult to reject, followed by disturbances 1 (in T_f) or 4 (in k_c^1). Disturbance 2 (in T_a) appears to have very little effect. δ_{13}, the CLDG for the effect of F_f on T_1 does not roll of at high frequencies. Some high frequency effect of F_f on T_1 must therefore be expected. This suggests the use of feedforward from F_f to F_s used together with feedback control for good disturbance rejection at high frequencies, unless F_f is controlled such that only slow changes in this variable can occur.
The predictions based on the CLDG's are verified by closed loop simulations, as demonstrated in Figure 5 for case 1. For our choice of manipulated variables, it is only unmodelled effects that limit the achievable bandwidth. We have therefore chosen to tune each loop to give a closed loop bandwidth for the loop of approximately one minute. This results in the following controller

$$c_1(s) = 1.23\frac{0.56s + 1}{0.56s} \tag{33}$$

$$c_2(s) = 0.5\frac{s + 1}{s} \tag{34}$$

These controller tunings result in a sensitivity function S with no peak. In Figure 6 we have for each disturbance plotted the ratio of the magnitude of the transfer function from disturbance to T_{rg} when the above controller is used relative to the magnitude of the transfer function from disturbance to T_{rg} for the open loop system. The assertion made earlier that good control of T_1 will also limit the offset in T_{rg} is shown to hold. The amplification of the effect of disturbances 1 and 3 (T_f and F_f) at high frequencies is of no significance as the magnitude of the open loop transfer function is very small at these frequencies.
Note that it is not meaningful to use the CLDG to choose between different choices of controlled output variables. For this reason, we have chosen to include the CLDG's only for the Hicks control structure.

8 Complete combustion mode

8.1 Choice of controlled variables

1) Conventional control structure, $y_{CC} = (T_1, O_f)^T$
For this choice of controlled variables we obtain no RHP transmission zero.

2) Kurihara control structure. $y_{KC} = (T_{rg}, O_f)^T$
For this choice of controlled variables we obtain an RHP transmission zero in the frequency range $0.2 - 0.4$ [rad/min].

We will therefore consider the conventional control structure in the following.

8.2 Pairing of controlled and manipulated variables.

The RGA for the pairing T_1-F_s, O_d-F_a approaches 1 at high frequencies, and is positive and quite small (2-3) at steady state for almost all operating points investigated.
The only exception is found in a region of high regenerator temperatures and low concentration of oxygen in the flue gas. In this region the RGA at low frequencies is negative and larger (ca. -9), whereas the RGA approaches 1 at high frequencies also in this region. This operating region should be avoided, as the low oxygen concentration in the flue gas indicates that the oxygen concentration in the dense bed is insufficient to convert all CO to CO_2 within the dense bed, and afterburning may therefore result. This problem is discussed further below.

8.3 Effect of changes in the operating point.

The transfer function matrix G_C is arranged according to

$$\begin{bmatrix} T_1 \\ O_f \end{bmatrix} = G_C \begin{bmatrix} F_s \\ F_a \end{bmatrix} \tag{35}$$

With the controlled variables chosen, most changes in the operating point are found to have a relatively small effect on the control of the FCC in the complete combustion mode. Although a number of operating points ("cases") have been studied, our findings can be illustrated by the results in Table 2. Case 1 in Table 2 gives a typical operating point.
Case 2 shows an unstable operating point, found in a region of high regenerator temperatures and low concentration of oxygen in the flue gas. We concluded above that this operating region should be avoided. The transfer function matrix G_C has a RHP pole at 7×10^{-4} [rad/min]. At this operating point there is also a pair of complex RHP transmission zeros in G_C at a frequency of 0.14 [rad/min]. The system is easily stabilized, e. g. by feedback from T_1 to F_s, but fast control of both T_1 and O_f will not be possible in this region. However, the drift into the unstable region is slow and a well designed control system should easily avoid this region.

8.4 Sensitivity to parametric uncertainty.

The FCC process appears to be relatively insensitive to parametric uncertainty in the complete combustion mode for our choice of controlled variables. Changes in the coke production rate (k_c) can make the system open loop unstable, but again we find that the system is easily stabilized by feedback.

8.5 Disturbances

The same scalings for the riser exit temperature and the disturbances used for the partial combustion mode are also used in the complete combustion mode. For O_f, scaling is used such that an output error of magnitude 1 corresponds to 0.1 mole%. The resulting CLDG's are shown in figure 7. Comparing figure 7 to figure 4, it is clear that a higher loop gain at low frequencies is required in the complete combustion mode than in the partial combustion mode in order to reject the effect of disturbances on T_1. Figure 7 also shows that rejecting disturbances in O_f will be relatively easy.

9 Sensitivity to input uncertainty

Skogestad and Morari (1987b) found that large RGA elements in *both* the plant and controller means that the system is sensitive to uncertainty in the manipulated variables. Thus a decentralized controller will give a system which is relatively insensitive to uncertainty in the manipulated variables as the RGA of the controller is 1. On the other hand the nominal system performance (i. e. without uncertainty) will be poor for plants with large RGA elements, as the controller cannot compensate for the strong directionality of the plant. Decouplers can give excellent nominal performance for plants with large RGA elements, but the RGA of the controller will be the same as the RGA of the plant, and the resulting system will therefore be sensitive to uncertainty in the manipulated variables. For the 2×2 control problem for the FCC process we have generally found quite small RGA values, meaning that it should be possible to design successful decoupler for this problem. The only exception occurs in the unstable operating region in the complete combustion mode, which we concluded above should be avoided.

10 Effect of model features

10.1 Afterburning

Inclusion of the simple model for afterburning in the partial combustion mode given in Eq. (23) allows considering T_{cy} as a controlled variable. The results in this paper demonstrates how controllability in the partial combustion mode is improved when T_{cy} is chosen as a controlled variable instead of $\Delta T_{rg} = T_{cy} - T_{rg} = c_t O_d$. The afterburning model is therefore very important. The results have proved to be relatively insensitive to the value of c_t, and it thus appears to be little need for modelling afterburning in more detail.

10.2 Model reduction

All the calculations above were based on a five state model. However, the dynamics of the oxygen in the regenerator and the temperature and coke concentration in the stripper are much faster than the dynamics of the temperature and coke concentration in the regenerator. We have found that the FCC model can be reduced to only two states by setting $\frac{dO_d}{dt}$, $\frac{dT_{st}}{dt}$ and $\frac{dC_{st}}{dt}$ equal to zero. The error introduced by this model reduction is

minor, the most important effect being that the RHP transmission zero for the Kurihara control structure appears at a slightly higher frequency for the two state model than for the five state model. The zeros for the individual model elements are also affected, but we have found no instance where this will affect the conclusions for control structure selection. A state space realization of the two state model for case 1 in Table 1 is given in the Appendix.

10.3 Air flow pattern in the regenerator

Errazu et al. (1979) found that the behavior of the regenerator is well described by a model which assumes that the oxygen in the regenerator dense bed is uniformly distributed. Other authors, e. g. Kurihara (1967) and Krishna and Parkin (1985) assumes the air to move in plug flow through the regenerator. We have studied the effect of this assumption on our results. Here we will only consider the partial combustion mode, as it is only in the partial combustion mode we have found the results on control structure selection to be affected by the assumption about the air flow pattern in the regenerator.
Kurihara assumes the oxygen leaving the regenerator dense bed to be at pseudo-steady state, and is calculated from the following equation

$$O_d = O_{in} exp\left[\frac{-WP_{rg}/F_a}{[1.06 \times 10^{10}/F_a^2 + 1/(k_{or} exp(-E_{or}/RT_{rg})C_{rc})]}\right] \tag{36}$$

R_{cb}, the rate of coke combustion is found from a mass balance with the oxygen consumed:
[4]

$$R_{cb} = \frac{F_a}{M_a}(O_{in} - O_d)\frac{4(1+\sigma)}{(1+\sigma)n + 2 + 4\sigma}M_c \tag{37}$$

The values of E_{or} and P_{rg} are taken from Denn (1986), whereas the value for k_{or} has been adjusted to give a steady state close to case 1 in table 1.
The results for the Hicks control structure in the partial combustion mode are summarized for two cases in Table 3. In case 1 the gain from F_a to T_{cy} is negative, and we have a negative RGA. The immediate effect of increasing F_a will be to increase O_d, and hence also T_{cy}. However, T_{rg} will also increase, and because O_d in Eq. (36) is a very strong function of T_{rg}, O_d eventually decreases to a value below its original value. We therefore get a negative steady state gain from F_a to T_{cy}. In case 2 in Table 3 the value of O_d is lower because of the higher T_{rg}. There is therefore less scope for further reduction of O_d, and the steady state gain from F_a to T_{cy} is positive, and we get a positive RGA.

Kurihara (1967) studied the Hicks control structure, but states that it is "incomplete" from a safety point of view, because it has incomplete feedback information with respect to the states T_{rg} and C_{rc}, which he states are the variables which govern FCC safety. The argument is supported by a closed loop simulation of the Hicks control structure in which

[4] It should be noted that Kurihara ignored the presence of hydrogen in the coke. Clearly, for the mass balance in (37) the presence of hydrogen in the coke, represented by the parameter n, is important. The omission of hydrogen in the mass balance is repeated by Denn (1986) in his presentation of the Kurihara model when he states that a ratio of CO_2 to CO of unity results in a value of $C_1 = 2$ in his equation (5.62a). The right hand side of eq. (5.62a) also need to be multiplied by $32/M_a$ to be correct.

the system goes unstable after the air blower saturates. The controller tunings used in the simulations are not provided.
These results are probably explained by the negative RGA found for case 1 in Table 3 which means that one of the control loops must be unstable for the overall closed loop system to be stable (Grosdidier et al., 1985). In Kurihara's simulation example it must therefore be the loop F_s-T_1 which is unstable, and the system therefore becomes unstable when the other input (F_a, the air blower) saturates. We have the following comments:

1. One can choose which control loop should be stable on its own, and one would therefore choose the control loop which is least likely to saturate as the stable loop.

2. One can use some of the independent variables which are not used for the primary control to avoid saturation in the primary loops. For instance, if one uses F_s to control T_1 and the regenerated catalyst slide valve is prone to saturate, one can use the feed preheat temperature T_f to reset the regenerated catalyst slide valve to a desired position. Alternatively, the task of avoiding saturation in the manipulated variables in the decentralized control system can be assigned to an MPC controller on top of the decentralized control system.

3. Kurihara's statement that T_{rg} and C_{rc} govern FCC safety ignores the correlation between T_1 and wet gas production. Thus a high value of T_1 may cause the wet gas compressor to surge despite good control of T_{rg}.

4. When using the Hicks control structure, the main need for adding a control loop to control T_{rg} arises because of the wish to avoid undesirable catalyst to oil ratios in the riser, with resulting adverse effects on product split. Thus when the cyclone temperature T_{cy} is controlled, the main incentive for controlling T_{rg} is economic, and not related to safety. Slower control of T_{rg} than T_{cy} and T_1 can therefore be tolerated. Our results on measurement selection for the 3×3 control problem show that if the Hicks control structure is used for the control of T_{cy} and T_1, one can add the control loop k_c-T_{rg} without introducing serious interaction provided the loop k_c-T_{rg} has a closed loop time constant of approximately 20 minutes or slower.

5. In our opinion the assumption of plug flow of air in the regenerator is naive, as strong backmixing occurs in the regenerator. (We do however realize that the assumption of uniformly distributed oxygen in the regenerator is also an idealization.)

6. Finally, Grosdidier's (1990a) statement that the Hicks control structure is preferred in industry for controlling FCC's in the partial combustion mode also indicates that instability because of saturation in the manipulated variables does not occur frequently, although we know that it is common to operate FCC's close to constraints. It may also indicate that the assumption of uniformly distributed oxygen in the regenerator is more reasonable.

11 Conclusion

Partial combustion mode.
A favorable selection of controlled variables is critical for good control of the FCC process. Both the conventional control structure, which has T_1 and ΔT_{rg} as controlled variables, and the Kurihara control structure, which has T_{rg} and ΔT_{rg} as controlled variables, have RHP transmission zeros which limit the achievable bandwidth. On the other hand, we get no RHP transmission zeros with the Hicks control structure, which has T_1 and T_{cy} as controlled variables. This choice of controlled variables is therefore preferable. The best pairing is T_1-F_s, T_{cy}-F_a, because this RGA for this pairing is close to 1 in the frequency range around the desired closed loop bandwidth.
The Hicks control structure corresponds to the current industrial practice for decentralized control of FCC's in the partial combustion mode (Grosdidier, 1990a), and in hindsight this control structure may appear obvious. The fact that the socalled conventional control structure was predominant for many years (Pohlenz, 1963, Lee and Weekman, 1976) makes it clear that it is not so obvious. To our knowledge, this paper is the first to demonstrate how controllability of the FCC process is affected by the choice of controlled variables.

Complete combustion mode.
T_1 and O_d should be chosen as controlled variables, as this choice of controlled variables give no RHP transmission zero. In contrast, choosing T_{rg} and O_d as controlled variables gives an RHP transmission zero in the frequency range 0.2-0.4 [rad/min]. The best pairing is T_1-F_s, O_d-F_a, as this corresponds to positive steady state RGA values and to RGA values close to 1 around the desired closed loop bandwidth.

Disturbances.
Both in the partial combustion mode and in the complete combustion mode the effect of disturbances in the feed oil rate on the riser exit temperature is most difficult to reject. Fortunately, the feed oil flowrate is usually controlled, but our results demonstrate that any deliberate change in this variable should be made slowly, or feedforward from F_f to F_s should be used.

Sensitivity to parametric uncertainty and changes in the operating point.
Our results on measurement selection and variable pairing appear relatively insensitive to parametric uncertainty and changes in the operating point.

Effect of model features.
1) The FCC process can be described fairly well with a second order model.
2) A model of the afterburning in the partial combustion mode is essential for a proper selection of measurements.
3) The negative steady state RGA obtained at some operating points in the partial combustion mode when assuming plug flow of air in the regenerator means that one of the control loops must be unstable on its own (at the same operating points) in order to have a stable closed loop system. However, in our opinion the assumption of plug flow of air in the regenerator is a poor one.

Nomenclature

FCC models:

Nominal parameter values are given in parentheses. When different values are used for the partial and complete combustion modes, the values are given as (partial combustion mode/complete combustion mode).

C_{cat} - Catalytic coke produced in riser, mass fraction
C_{rc} - Coke on regenerated catalyst, mass fraction
C_{sc} - Coke on catalyst leaving riser, mass fraction
C_{st} - Coke on catalyst in reactor (stripper), mass fraction
c_{pa} - Heat capacity of air ($1.074 kJ/kgK$)
c_{pc} - Heat capacity of catalyst ($1.005 kJ/kgK$)
c_{po} - Heat capacity of oil ($3.1355 kJ/kgK$)
c_{pD} - Heat capacity of steam ($1.9 kJ/kgK$)
$[COR]$ - Catalyst to oil ratio on a mass basis
c_t - Factor in Eq. (23) ($5555 K$/molefraction)
E_{cf} - Activation energy for coke formation ($41.79 kJ/mole / 20.00 kJ/mole$)
E_{cb} - Activation energy for coke combustion assuming uniformly distributed oxygen in the regenerator ($158.59 kJ/mole$).
E_f - Activation energy for the cracking of gas oil ($101.5 kJ/mole$)
E_g - Activation energy for the cracking of gasoline
($112.6 kJ/mole$)
E_{or} - Activation energy for coke combustion assuming plug flow of air in the regenerator ($146.4 kJ/mole$).
F_a - Flowrate of air to the regenerator ($25.35 \frac{kg}{s} / 28.0 \frac{kg}{s}$)
F_f - Feed oil flowrate ($40.63 kg/s$)
F_s - Flow rate of regenerated catalyst ($294 kg/s$)
$\hat{F}_s$ - Flowrate of spent catalyst (assumed $= F_s$).
k_1 - Reaction rate constant for the total rate of cracking of gas oil ($9.6 \times 10^5 s^{-1}$)
k_2 - Reaction rate constant for the rate of cracking of gas oil to gasoline ($7.2 \times 10^5 s^{-1}$)
k_3 - Reaction rate constant for the rate of cracking of gasoline to light gases/carbon ($4.22 \times 10^5 s^{-1}$)
k_c - Reaction rate constant for the production of coke ($0.019 s^{-1} / 0.0093 s^{-1}$)
k_{cb} - Reaction rate constant for coke combustion assuming uniformly distributed oxygen in the regenerator ($2.077 \times 10^8 s^{-1}$).
k_{or} - Reaction rate constant for coke combustion assuming plug flow of air in the regenerator($58.29 m^2/($
M_a - Molecular weight of air (28.8544)
M_c - Bulk molecular weight of coke (14)
m - Factor for the dependence of the initial catalyst
activity on C_{rc} (80)
n - Number of moles of hydrogen per mole of carbon
in the coke (2)
N - Exponent for the dependence of C_{cat} on C_{rc} (0.4/0.0)
O_d - Concentration of oxygen in gas leaving regenerator dense bed, molefraction
O_{in} - Concentration of oxygen in air to regenerator (0.2136 molefraction)
R - Universal gas constant

R_{cb} - Rate of coke combustion (kg/s)
P_{rg} - Regenerator pressure ($172000 N/m^2$)
T_0 - Temperature at riser entrance
T_1 - Temperature at riser exit
T_a - Temperature of air to the regenerator
T_{cy} - Regenerator cyclone temperature
T_{st} - Temperature in reactor (stripper)
T_f - Feed oil temperature
t_c - Residence time in riser ($9.6s$)
W - Holdup of catalyst in regenerator ($176000kg$)
W_a - Holdup of air in the regenerator ($20kmol$)
W_{st} - Holdup of catalyst in stripper ($17500kg$)
y_f - Mass fraction of gas oil
y_g - Mass fraction of gasoline
z - Dimensionless distance along riser
α - Catalyst deactivation constant ($0.12s^{-1}$)
α_2 - Fraction of the gas oil that cracks which cracks to gasoline, $k_2/k_1 = 0.75$.
ΔH_{cb} - Heat of combustion of coke ($kJ/kmol$)
ΔH_f - Heat of cracking ($506.2kJ/kg$)
λ - Mass flowrate of dispersion steam / mass flowrate of feed oil (0.035)
σ - Molar ratio of CO_2 to CO in the regenerator dense bed
ϕ_0 - Initial catalyst activity at riser entrance
Θ - Dimensionless temperature in riser

Control analysis:
$C(s)$ - Diagonal controller transfer function matrix
$c_i(s)$ - Controller element for output i
$d(s)$ - Vector of disturbances.
$e(s) = y(s) - r(s)$ - Vector of output errors
$G(s)$ - Process transfer function matrix
$G_P(s)$ - Transfer function matrix for the partial combustion mode defined by Eq. (32)
$G_C(s)$ - Transfer function matrix for the complete combustion mode defined by Eq. (35)
$G_d(s)$ - Disturbance transfer function matrix
$g_{ij}(s)$ - ij'th element of $G(s)$
$g_{dik}(s)$ - ik'th element of $G_d(s)$
$r(s)$ - Reference signal for outputs
$S(s)$ - Sensitivity function $S = (I + GC)^{-1}$
$u(s)$ - Vector of manipulated inputs.
$y(s)$ - vector of outputs
$\Delta(s)$ - Closed loop disturbance gain matrix
$\delta_{ik}(s)$ - ij'th element of $\Delta(s)$
$\Lambda(s)$ - Relative gain matrix
$\lambda_{ij}(s)$ - ij'th element of $\Lambda(s)$
ω - Frequency
ω_B - Closed loop bandwidth

References

Bristol, E. H. (1966). On a new measure of interactions for multivariable process control. *IEEE Trans. Automat. Control*, AC-11, 133-134.

Bristol, E. H. (1978). Recent results on interactions in multivariable process control. Paper at *AIChE Annual Meeting*, Chicago, IL.

Denn, M. M. (1986). *Process Modeling.* John Wiley & Sons, Inc., New York.

Errazu, A. F., DeLasa, H. I. and Sarti, F. (1979). A fluidized bed catalytic cracking regenerator model, grid effects. *Can. J. Chem. Eng.*, 57, 191-197.

Grosdidier, P., Morari, M. and Holt, B. R. (1985). Closed loop properties from steady state gain information. *Ind. Eng. Chem. Fundam.*, 24, 221-235.

Grosdidier, P. (1990a). Personal communication.

Grosdidier, P. (1990b). Analysis of interaction direction with the singular value decomposition. *Computers chem. Engng.*, 6, 687-689.

Grosdidier, P., Mason, A., Aitolahti, A., Heinonen, P. and Vanhamäki, V. (1991). FCC unit reactor-regenerator control. Submitted to *Journal of Process Control.*

Hicks, R. C., Worrell, G. R. and Durney, R. J. (1966). Atlantic seeks improved control; studies analog-digital models. *The Oil and Gas Journal*, Jan. 24, 97-105.

Hovd, M. and Skogestad, S. (1991). Use of frequency-dependent RGA for control system analysis, structure selection and design. Submitted to *Automatica.*

Kurihara, H. (1967). Optimal control of fluid catalytic cracking processes. *Ph.D. Thesis* MIT.

Krishna, A. S. and Parkin, E. S. (1985). Modeling the regenerator in commercial catalytic cracking units. *Chem. Eng. Prog.*, 81, 4, 57-62.

Lee, E. and Groves, F. R. (1985). Mathematical model of the fluidized bed catalytic cracking plant. *Trans Soc. Comp. Sim.*, 2, 219-236.

Lee, W. and Weekman, V. W. (1976). Advanced control practice in the chemical process industry: A view from industry. *AIChE Journal*, 22, 27-38.

Ljungquist, D. (1990). Online estimation in nonlinear state space models with application to catalytic cracking. *Dr. ing. Thesis*, Norwegian Institute of Technology.

McAvoy, T. J. (1983). *Interaction Analysis*, Instrument Society of America, Research Triangle Park, USA.

Morari, M. and Zafiriou, E. (1989). *Robust Process Control.* Prentice Hall, Englewood Cliffs, NY.

Pohlenz, J. B., (1963). How operational variables affect fluid catalytic cracking. *Oil and Gas Journal*, April 1.

Rheaume, L., Ritter, R. E., Blazek, J. J. and Montgomery, J. A., (1976). Two new carbon monoxide oxidation catalysts get commercial tests. *Oil and Gas Journal*, May 24.

Shah, Y. T., Huling, G. P., Paraskos, J. A. and McKinney, J. D. (1977). A kinematic model for an adiabatic transfer line catalytic cracking reactor. *Ind. Eng. Chem. Proc. Des. Dev.*, 16, 89-94.

Shinskey, F. G. (1967). *Process Control Systems*, McGraw Hill, New York.

Shinskey, F. G. (1984). *Distillation Column Control*, 2nd Edition, McGraw Hill, New York.

Skogestad, S. and Hovd, M. (1990). Use of frequency dependent RGA for control structure selection. *American Control Conference*, San Diego CA.

Skogestad, S. and Morari, M. (1987a). Effect of disturbance direction on closed loop performance. *Ind. Eng. Chem. Res.*, 26, 2029-2035.

Skogestad, S. and Morari, M. (1987b). Implications of large RGA elements on control performance. *Ind. Eng Chem. Res.*, 26, 11, 2323-2330.

Weekman, V. W. and Nace, D. M. (1970). Kinetics of catalytic cracking selectivity in fixed, moving and fluid bed reactors. *AIChE Journal*, 16, 397-404.

Appendix

Two state model for the FCC in the partial combustion mode (Case 1 in Table 1):

$$\frac{dx}{dt} = Ax + Bu + Ed \tag{38}$$

$$y = Cx + Du + Fd \tag{39}$$

$$A = \begin{bmatrix} -2.55 \times 10^{-2} & 1.51 \times 10^{-6} \\ 227 & -4.10 \times 10^{-2} \end{bmatrix} \tag{40}$$

$$B = \begin{bmatrix} 3.29 \times 10^{-6} & -2.60 \times 10^{-5} \\ -2.80 \times 10^{-2} & 7.80 \times 10^{-1} \end{bmatrix} \tag{41}$$

$$C = \begin{bmatrix} 1.32 \times 10^{3} & 0.559 \\ -4.42 \times 10^{3} & 0.538 \\ 0 & 1 \end{bmatrix} \tag{42}$$

$$D = \begin{bmatrix} 0.362 & 0 \\ 0 & 0.877 \\ 0 & 0 \end{bmatrix} \tag{43}$$

$$E = \begin{bmatrix} 6.87 \times 10^{-7} & 0 & -7.06 \times 10^{-6} & 3.53 \times 10^{-2} \\ 2.47 \times 10^{-2} & 9.24 \times 10^{-3} & -2.54 \times 10^{-1} & 0 \end{bmatrix} \tag{44}$$

$$F = \begin{bmatrix} 0.246 & 0 & -0.253 & 0 \\ 0 & 0 & 0 & 0 \\ 0 & 0 & 0 & 0 \end{bmatrix} \tag{45}$$

$$
\begin{aligned}
y &= \begin{bmatrix} T_l \\ T_{cy} \\ T_{rg} \end{bmatrix} \\
x &= \begin{bmatrix} C_{rc} \\ T_{rg} \end{bmatrix} \\
u &= \begin{bmatrix} F_s \\ F_a \end{bmatrix} \\
d &= \begin{bmatrix} T_f \\ T_a \\ F_f \\ k_c \end{bmatrix}
\end{aligned}
\tag{46}
$$

TABLE 1. Operating Points used in Section 7 for the partial combustion mode.

	Case 1	Case 2
T_{rg}	965.4 K	966.6 K
T_1	776.9 K	770.6 K
T_{cy}	988.1 K	997.4 K
C_{rc}	5.207×10^{-3}	3.578×10^{-3}
$G_P(0)$	$\begin{pmatrix} 0.5587 & 10.16 \\ -0.5577 & 10.35 \end{pmatrix}$	$\begin{pmatrix} 0.3893 & 10.83 \\ -0.7606 & 8.22 \end{pmatrix}$
RGA(0)	0.505	0.280
RHP zeros [rad/min]		
Multivariable	–	–
In elements	$\begin{pmatrix} - & - \\ - & - \end{pmatrix}$	$\begin{pmatrix} - & - \\ - & - \end{pmatrix}$

- denotes that no RHP-zero is present at frequencies below 100 [rad/min].

TABLE 2. Operating points used in Section 8 for the complete combustion mode.

	Case 1	Case 2
T_{rg}	998.4 K	1012.3 K
T_1	788.0 K	797.3 K
O_d	1.038×10^{-2}	3.098×10^{-3}
C_{rc}	9.645×10^{-3}	2.527×10^{-3}
$G_C(0)$	$\begin{pmatrix} 29.98 & -11.23 \\ -0.001875 & 0.01210 \end{pmatrix}$	$\begin{pmatrix} -11.23 & 84.18 \\ 0.004131 & -0.02798 \end{pmatrix}$
RGA(0)	2.38	-9.3
RHP zeros [rad/min]		
Multivariable	–	0.014
In elements	$\begin{pmatrix} - & 0.018 \\ - & - \end{pmatrix}$	$\begin{pmatrix} - & 0.0007 \\ 1 & 0.08 \end{pmatrix}$

TABLE 3. Operating Points used in Section 10.3 assuming plug flow of air in the regenerator.
(Partial combustion mode)

	Case 1	Case 2
T_{rg}	966.1 K	983.2 K
T_1	777.3 K	783.7 K
T_{cy}	987.3 K	993.1 K
C_{rc}	5.039×10^{-3}	4.409×10^{-3}
$G_P(0)$	$\begin{pmatrix} 2.907 & 36.72 \\ -5.562 & -45.73 \end{pmatrix}$	$\begin{pmatrix} 0.695 & 12.72 \\ -1.125 & 5.306 \end{pmatrix}$
RGA(0)	−1.87	0.205
RHP zeros [rad/min]		
Multivariable	–	–
In elements	$\begin{pmatrix} - & - \\ - & 0.025 \end{pmatrix}$	$\begin{pmatrix} - & - \\ - & - \end{pmatrix}$

Figures

1. **Fig. 1.** Schematic overview of an FCC plant.

2. **Fig. 2.** Schematic representation of a hierarchical control system.

3. **Fig. 3.** Block diagram of controller and plant

4. **Fig. 4.** Closed loop disturbance gains, δ_{ik}, for the control structure chosen in section 7.2 for the partial combustion mode. i denotes output and k disturbance. The loop gains resulting from the controller used in Fig. 5 are shown with dashed lines.

5. **Fig. 5.** Closed loop simulation of the effect of disturbances for the partial combustion mode using the controller in section 7.5. A 5 K increase in T_a enters at 60 minutes, 5 K decrease in T_f at 180 minutes, 2.5% increase in k_c^1 at 300 minutes and a 4 kg/s decrease in F_f enters at 420 minutes.

6. **Fig. 6.** Ratio of the magnitude of the transfer function from disturbance to T_{rg} for the closed loop system using the controller in section 7.5 relative to the magnitude of the open loop transfer function.

7. **Fig. 7.** Closed loop disturbance gains, δ_{ik}, for the control structure chosen in section 8.2 for the complete combustion mode. i denotes output and k disturbance.

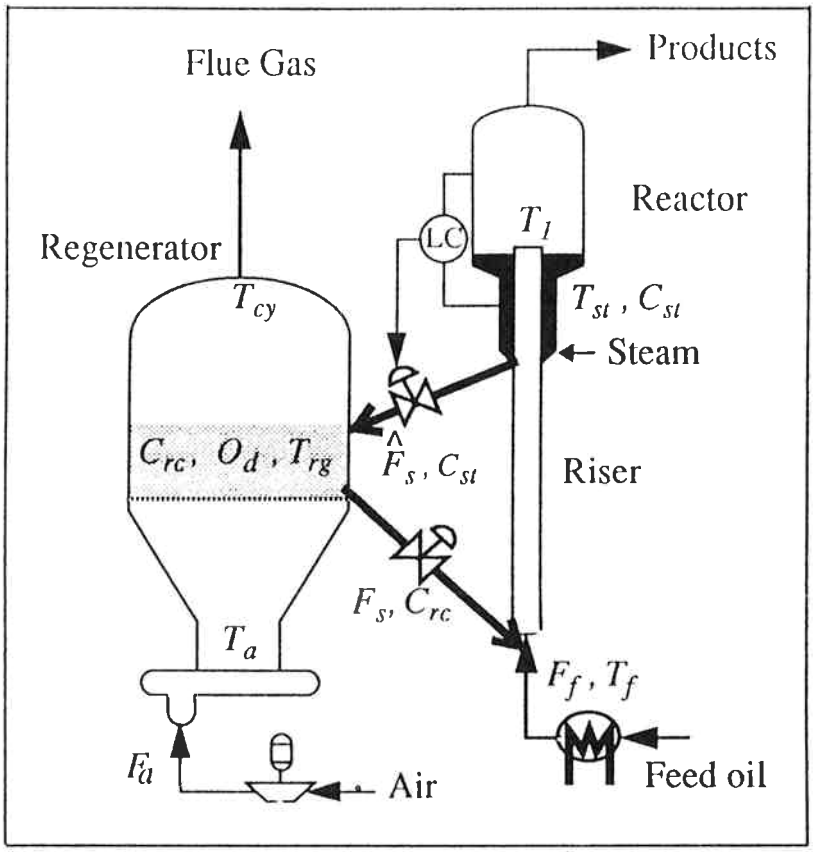
Flue Gas
Products
Regenerator
Reactor
LC
T_1
T_{cy}
T_{st} , C_{st}
Steam
C_{rc}, O_d , T_{rg}
$\hat{F}_s$, C_{st}
Riser
F_s, C_{rc}
T_a
F_f , T_f
F_a
Air
Feed oil

Fig. 1.

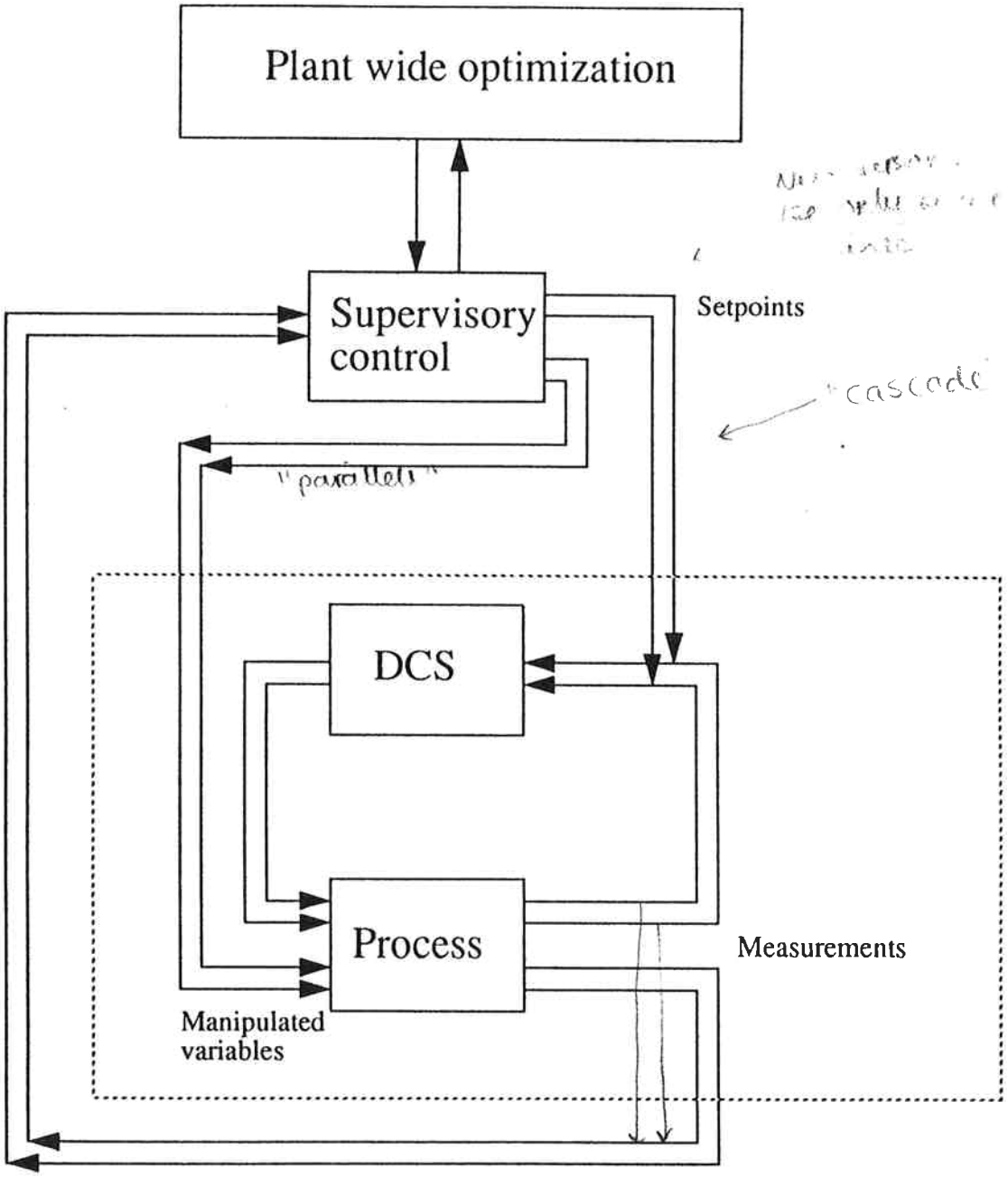
Plant wide optimization
Supervisory control
Setpoints
DCS
Process
Measurements
Manipulated variables

Fig. 2.

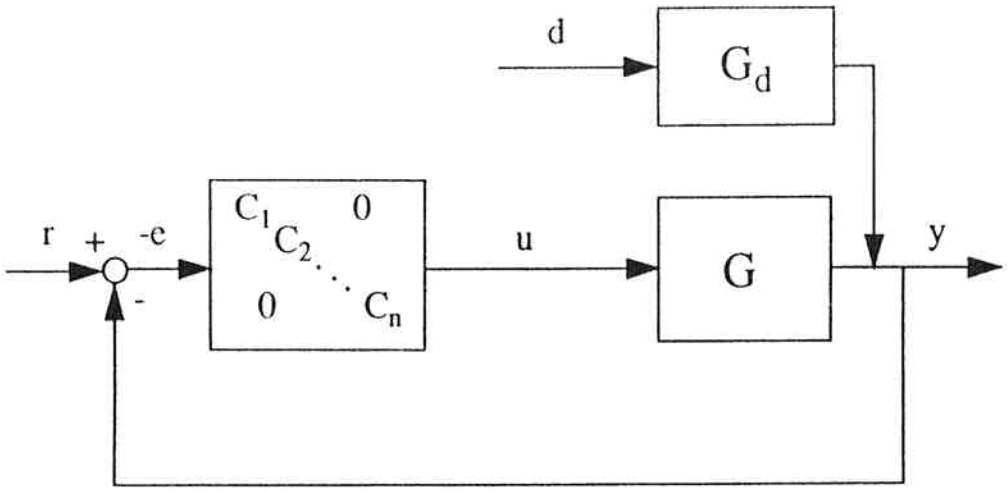

Fig. 3.

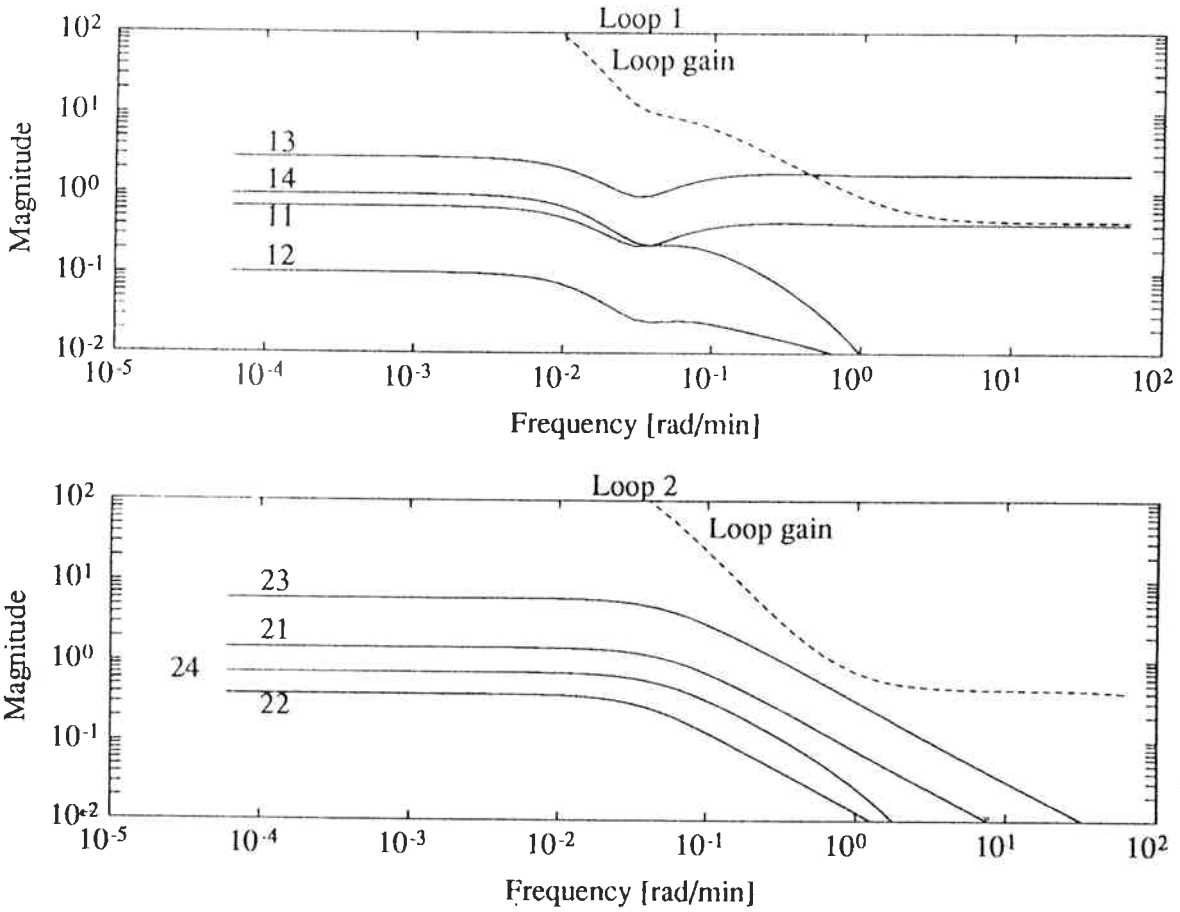
Loop 1
Loop gain
13
14
11
12
Magnitude
Frequency [rad/min]
Loop 2
Loop gain
23
21
24
22
Magnitude
Frequency [rad/min]

Fig. 4.

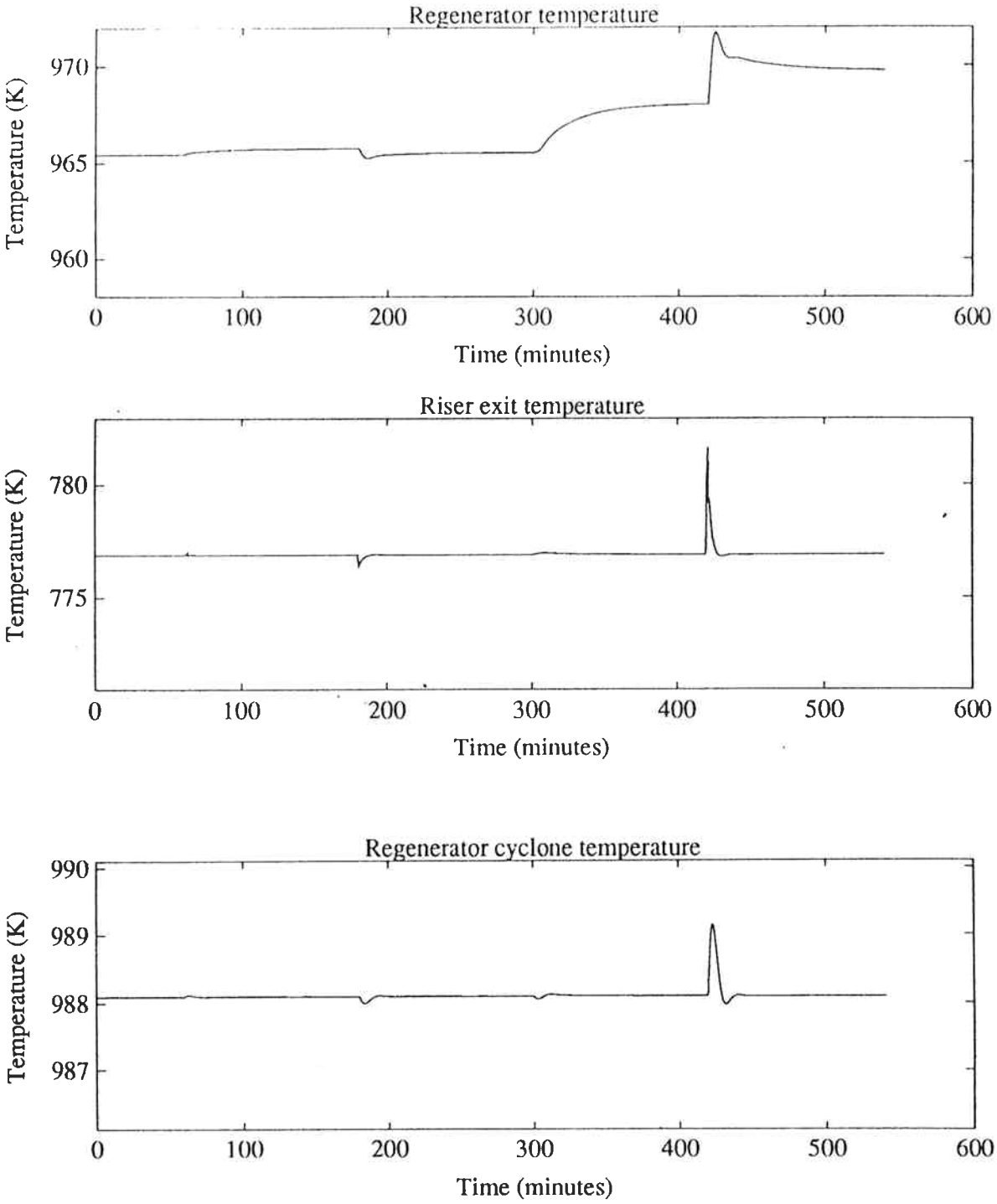
Regenerator temperature
Temperature (K)
970
965
960
0
100
200
300
400
500
600
Time (minutes)
Riser exit temperature
Temperature (K)
780
775
0
100
200
300
400
500
600
Time (minutes)
Regenerator cyclone temperature
Temperature (K)
990
989
988
987
0
100
200
300
400
500
600
Time (minutes)

Fig. 5.

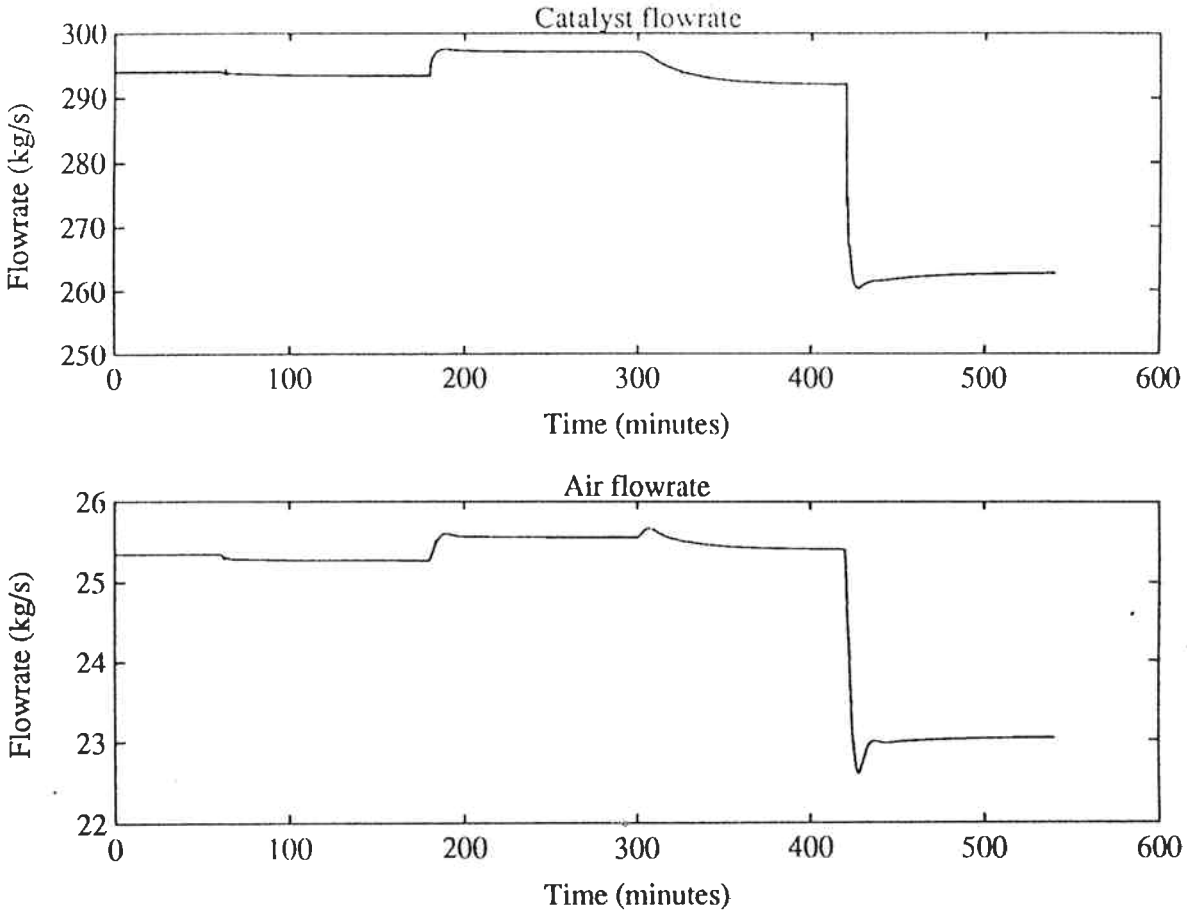

Fig. 5 continued.

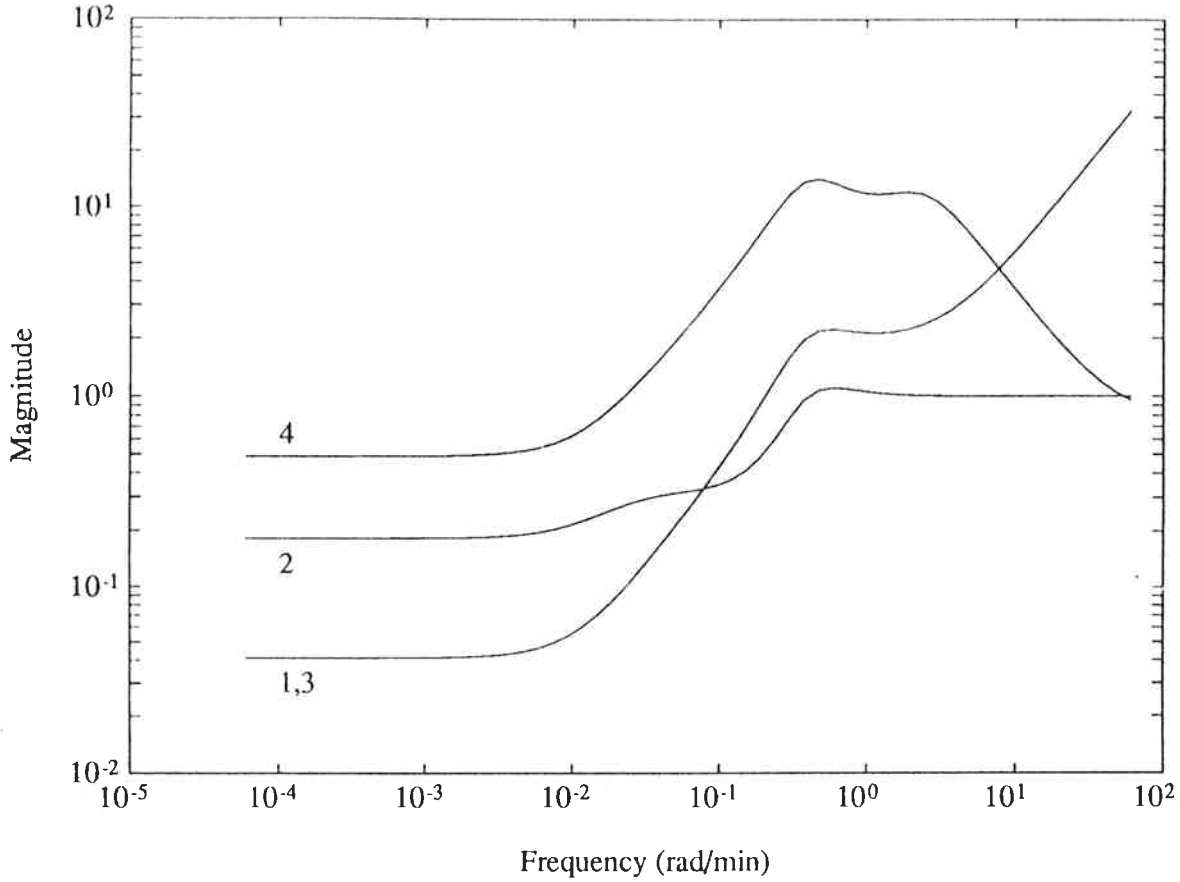
Magnitude
10^2
10^1
10^0
10^{-1}
10^{-2}
4
2
1,3
10^{-5}
10^{-4}
10^{-3}
10^{-2}
10^{-1}
10^0
10^1
10^2
Frequency (rad/min)

Fig. 6.

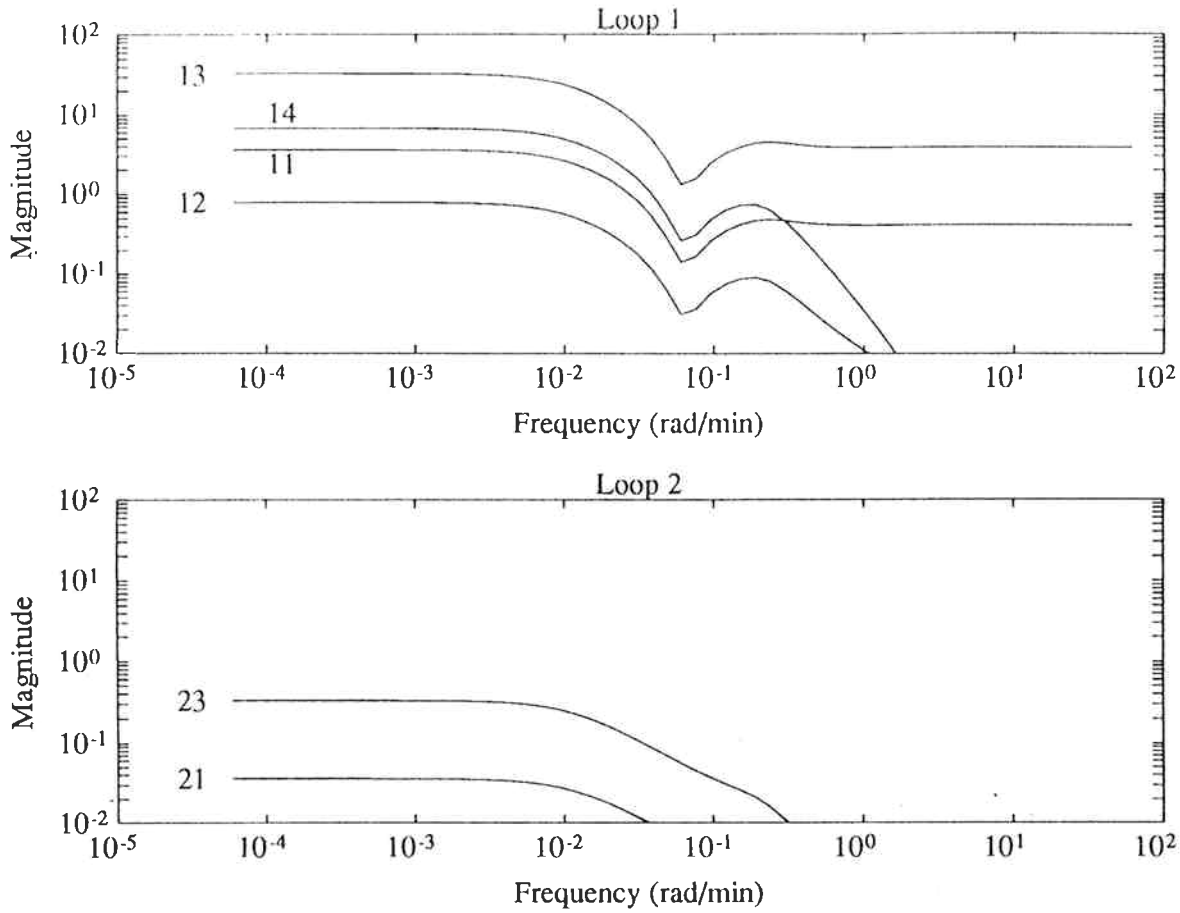
Loop 1
Magnitude
10^2
10^1
10^0
10^{-1}
10^{-2}
13
14
11
12
10^{-5}
10^{-4}
10^{-3}
10^{-2}
10^{-1}
10^0
10^1
10^2
Frequency (rad/min)
Loop 2
Magnitude
10^2
10^1
10^0
10^{-1}
10^{-2}
23
21
10^{-5}
10^{-4}
10^{-3}
10^{-2}
10^{-1}
10^0
10^1
10^2
Frequency (rad/min)

Fig. 7.